INSTITUTE OF PHYSICS PUBLISHING JOURNAL OF PHYSICS D: APPLIED PHYSICS
J. Phys. D: Appl. Phys. **38** (2005) 127–134 doi:10.1088/0022-3727/38/1/020

Improving reliability of modelling heat and fluid flow in complex gas metal arc fillet welds—part II: application to welding of steel

A Kumar and T DebRoy

Department of Materials Science and Engineering, The Pennsylvania State University, University Park, PA 16802, USA

Received 26 July 2004, in final form 16 November 2004
Published 16 December 2004
Online at stacks.iop.org/JPhysD/38/127

Abstract
In order to improve the reliability of numerical calculations of heat and fluid flow in fusion welding, a model was proposed in part I of this paper to determine the uncertain welding input parameters from a limited volume of experimental data. The application of the model for the complex gas metal arc (GMA) fillet welding of mild steel is reported in this part of the paper. The values of the arc efficiency, effective thermal conductivity and effective viscosity were evaluated as a function of the heat input. A vorticity-based mixing-length hypothesis was also used to independently calculate the values of the effective viscosity and effective thermal conductivity. Good agreement was obtained between the values of these parameters calculated using the two techniques, indicating the effectiveness of the proposed model in improving the reliability of heat and fluid flow calculations in fusion welding. The shape and size of the fusion zone, finger penetration characteristic of the GMA welds and solidified free surface profile computed using the optimized values of the uncertain welding parameters were in fair agreement with the corresponding experimental results for various welding conditions. In particular, the computed values of the leg length, the penetration depth and the actual throat agreed well with those measured experimentally for various heat inputs.

1. Introduction

In recent years, phenomenological models of fusion welding have provided valuable understanding of the welding processes [1–8] and welded materials [9–15]. These models have been useful in quantitatively understanding the underlying physics of the process [1–8, 16] and in examining the influence of different physical phenomena [16] and process parameters [1–5] on the welding processes. Although these models use the time-tested fundamental equations of conservation of mass, momentum and energy with appropriate boundary conditions, their predictions are affected by the uncertainty in the values of various input parameters used in the modelling [3, 4, 17]. For example, the reported values of arc efficiency vary significantly for apparently similar welding conditions, reflecting the complexity of the gas metal arc (GMA) welding process. Furthermore, the GMA welding process is characterized by strong convection currents driven to a large extent by the electromagnetic and Marangoni forces and to a much lesser extent by the buoyancy and other forces. During linear welding, the temperature and velocity fields in the weld pool often do not change appreciably except at the beginning and the end of the welding. In these quasi-steady weld pools, local velocities typically have two components, a time-independent or steady mean velocity and a time-dependent or fluctuating velocity. The convective heat and mass transport in the weld pool are affected by both the mean and the fairly significant fluctuating velocities that are present in the weld pool. The contribution of the fluctuating velocities to the convective heat and mass transfer

is considered in the calculations by enhancing the values of thermal conductivity and viscosity to account for the enhanced heat and mass transfer. Unlike the molecular values of the thermal conductivity and viscosity, the enhanced values of these 'transport properties' are not physical properties of the fluid and, as a result, their values cannot be obtained from the standard compilations of thermophysical properties. In contemporary transport phenomena, the enhanced values of transport properties are calculated using an appropriate turbulence model.

The momentum transport rates in the weld pool owing to the strong recirculating velocities with fluctuating components are often taken into account [1, 2, 5–12] by simple 'zero-equation' or algebraic turbulence models. In these calculations, the effects of turbulence are simulated by arbitrarily enhancing the molecular values of thermal conductivity and viscosity by ten to 100 times. The values of the enhanced viscosity and thermal conductivity are properties of the specific welding system and cannot be easily assigned from fundamental principles. Although the established turbulence models often serve as a basis for the estimation of enhanced transport properties, the empirical constants in these models have been determined using experimental data from large-scale parabolic flows. In contrast, fluid flow in the weld pool is strongly recirculatory or elliptic in nature, and the size of the weld pool is rather small. Currently there is no unified basis for accurately prescribing the values of the effective thermal conductivity, effective viscosity and arc efficiency. The values of these parameters significantly affect the results of numerical heat transfer and fluid flow calculations.

The present work seeks to enhance the reliability of the heat and mass transfer calculations in the weld pool by determining how the uncertain input parameters, i.e. the arc efficiency, the effective thermal conductivity and the effective viscosity, vary with heat input. The values of these parameters are determined from a limited volume of experimentally measured weld pool penetration, throat and leg length data using a combination of an optimization algorithm and a numerical heat transfer and fluid flow model. Part I of this paper explains how two interactive computational modules are embedded into the present model—one for the analysis of heat transfer and fluid flow in fusion welding and the other for the optimization. In effect, the procedure identifies values of uncertain parameters for each set of welding conditions in an iterative manner, starting from a set of their initial guessed values.

The manners in which the turbulent viscosity and turbulent thermal conductivity vary spatially in the weld pool due to spatial variation of heat distribution on the workpiece are analysed based on a vorticity-based mixing-length turbulence model. The proposed vorticity-based turbulence model uses a variable mixing-length to adequately consider an irregular and complex weld pool geometry characterized by finger penetration and severe deformation of the weld pool under the arc. Furthermore, it is algebraic in form and, therefore, significantly less computationally intensive than the k–ε turbulence model that contains several empirical constants determined from large-scale parabolic flow experiments. Hong *et al* [15] have shown that a vorticity-based mixing-length approach can satisfactorily describe enhancement of transport properties and convective heat transport in hemispherical GTA weld pools. Although the vorticity-based variable mixing-length calculations proposed in this paper provide a useful method for the heat transfer and fluid flow calculations in the weld pool, their applications are computationally more intensive than the use of effective transport properties. Therefore, the model extracts the effective values of the transport properties from a limited volume of experimental data and enhances the reliability of the heat and fluid flow calculations in the weld pool by determining how the uncertain input parameters, i.e. the arc efficiency, the effective thermal conductivity and the effective viscosity, vary with heat input.

2. Results and discussion

The evolution of the weld pool involves a complex interaction of physical processes such as the application of the welding arc, metal droplet transfer, heat transfer through conduction and convection, free surface deformation and the fluid flow inside the weld pool. To simulate these simultaneous processes correctly in the numerical heat transfer and fluid flow analysis, the values of the arc efficiency (η), effective thermal conductivity (k_e) and effective viscosity (μ_e) are needed. The following section shows the effects of these parameters on the geometry of the weld pool.

2.1. Effects of effective thermal conductivity, viscosity and arc efficiency

The effects of variation of the effective thermal conductivity and arc efficiency on the non-dimensional weld geometry, i.e. leg length, throat and penetration, are shown in figures 1(*a*)–(*c*) for case #1 listed in table 1. The non-dimensional values of the leg length, throat and penetration shown in these figures are obtained by dividing the numerically computed values with the corresponding experimentally obtained values. The increase in k_e leads to a higher heat conduction rate inside the weld pool and, consequently, results in a lower temperature gradient. Since most of the heat flows downwards, the value of the leg length decreases with an increase in k_e for a fixed value of arc efficiency as shown in figure 1(*a*). However, when the arc efficiency is increased, from 0.40 to 0.75, an about 25% increase in the non-dimensional leg length is achieved because the leg length depends mainly on the heat input from the arc.

In contrast to the leg length, the penetration is significantly affected by the heat transfer due to impinging metal droplets. The sensible heat of the droplets is distributed mainly to a region directly under the arc, and it affects the penetration. The enhanced thermal conductivity improves the heat transfer rate. The more efficient distribution of a given amount of heat from the droplets in all directions leads to a smaller penetration as shown in figure 1(*b*). This figure also shows that the penetration increases with increase in heat input as expected. Figure 1(*c*) shows that the computed non-dimensional throat does not vary significantly with either the arc efficiency or the effective thermal conductivity for a given wire feed rate and welding speed. This behaviour is also expected since the size of the throat is affected by the rate of mass addition. Furthermore, the weld pool dimensions decrease with an increase in the value

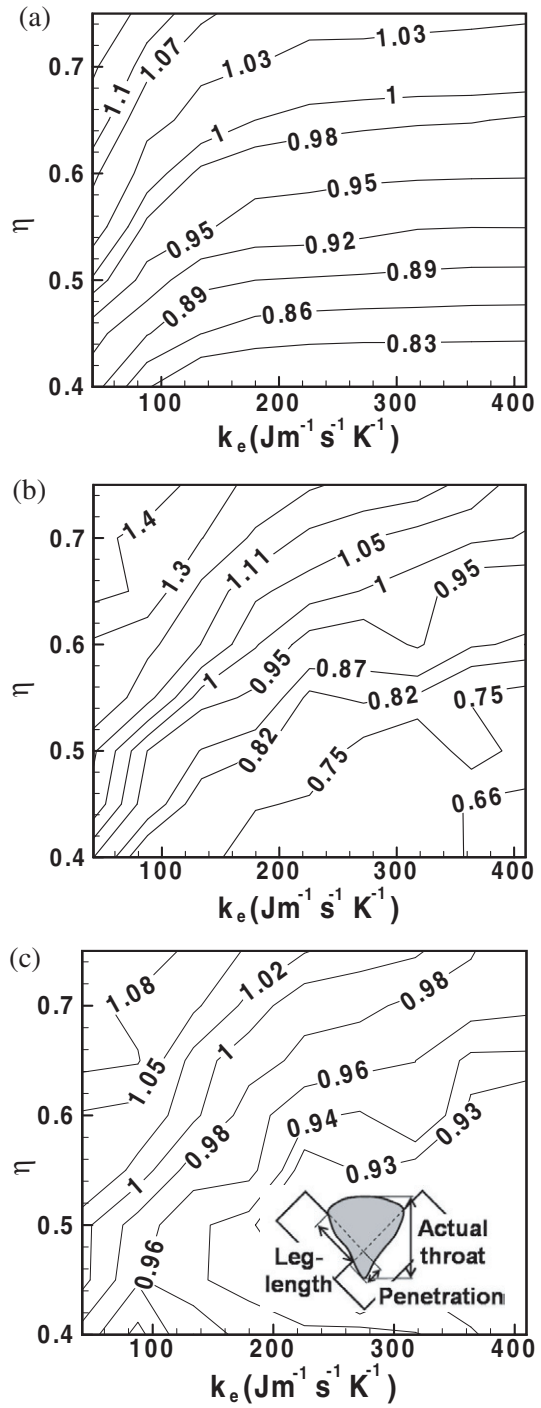

Figure 1. Contour plot of (*a*) non-dimensional leg length, (*b*) non-dimensional penetration and (*c*) non-dimensional throat for various values of arc efficiency (η) and effective thermal conductivity (k_e) for case #1 listed in table 1.

of the effective viscosity for a fixed value of the arc efficiency due to a retardation in convective flow [18]. The trends shown in figures 1(*a*), (*b*) and (*c*) were also true for other values of current, voltage, wire feed rate, CTWD and welding speed investigated.

Figures 1(*a*), (*b*) and (*c*) show that there are several independent combinations of η and k_e that would result in good agreement between the computed and the experimental

Table 1. Welding conditions used in the experiments.

No.	Contact tube to workpiece distance, CTWD (mm)	Wire feeding rate (mm s^{-1})	Travel speed (mm s^{-1})	Voltage (V)	Estimated current (A)
1	22.2	169.3	4.2	31	312.0
2	22.2	211.7	6.4	31	362.0
3	22.2	169.3	6.4	33	312.0
4	22.2	211.7	4.2	33	362.0
5	28.6	169.3	6.4	31	286.8
6	28.6	169.3	4.2	33	286.8
7	28.6	211.7	4.2	31	331.4
8	28.6	211.7	6.4	33	331.4
9	25.4	190.5	5.3	29.6	322.6
10	25.4	190.5	5.3	34.4	322.6
11	25.4	190.5	7.8	32.0	322.6
12	25.4	240.8	5.3	32.0	375.6

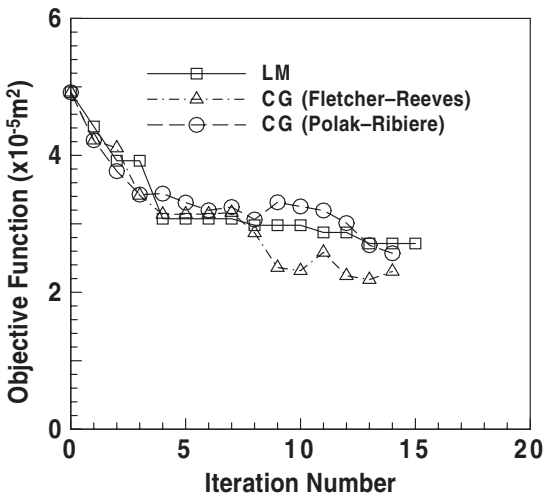

Figure 2. Computed values of the objective function, O($\boldsymbol{f}$), using the LM method and the two versions of the CG method as a function of the iteration number.

values of the leg length, penetration or throat. However, there is no guarantee that the same combination of η and k_e would lead to satisfactory prediction of all weld dimensions given by $p_m^* = t_m^* = 1_m^* = 1$. An optimum set of values of the arc efficiency (η), effective thermal conductivity (k_e) and effective viscosity (μ_e) are required to correctly predict the weld bead geometry and improve the reliability of the results obtained using numerical heat transfer and fluid flow models.

2.2. Optimized values of effective thermal conductivity, viscosity and arc efficiency

Figure 2 depicts the variation in the objective function (i.e. O($\boldsymbol{f}$)) with the number of iterations. The objective function decays rapidly in the first four iterations in the Levenberg–Marquardt (LM) method and both versions of the conjugate gradient (CG) method. After that, the objective function becomes almost constant for several iterations and then starts fluctuating. Figure 2 shows that the CG method of Fletcher and Reeves gives a somewhat better convergence of the objective function compared with the other two methods. In the CG method of Fletcher and Reeves, the minimum value of the

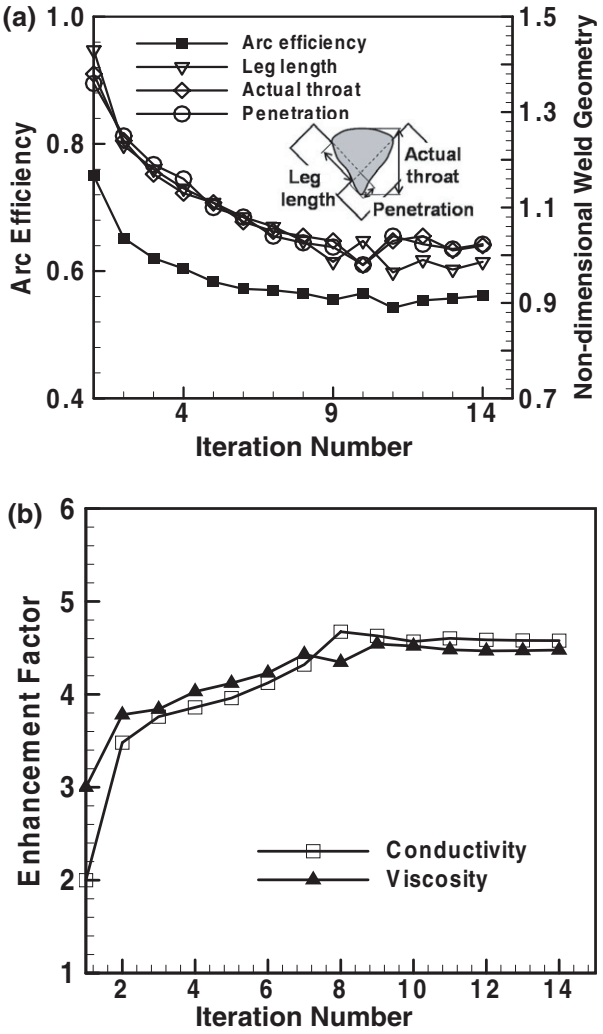

Figure 3. Optimized values of (*a*) arc efficiency (represented on left side vertical axis) and non-dimensional weld dimensions (represented on right side vertical axis) and (*b*) enhancement factor of thermal conductivity (i.e. $f_k^e = k_e/k_L$) and viscosity (i.e. $f_\mu^e = \mu_e/\mu_L$) using the Fletcher–Reeves' CG method for case #2 of table 1.

objective function obtained is 0.22 after 13 iterations, while LM and Polak–Ribiere's CG method produced values of 0.27 and 0.26 in 13 and 14 iterations, respectively. Therefore, the final optimized values of the arc efficiency, effective thermal conductivity and effective viscosity are calculated using Fletcher and Reeves' CG method.

Figures 3(*a*) and (*b*) show the variation in the values of the non-dimensional weld dimensions, arc efficiency, enhancement factor for thermal conductivity ($f_k^e = k_e/k_L$) and viscosity ($f_\mu^e = \mu_e/\mu_L$) with iterations for case #2 in table 1. Figure 3(*a*) shows that the non-dimensional weld geometrical parameters are initially very large due to the large value of the assumed arc efficiency. However, as the calculation progresses, the weld dimensions decrease and tend to attain the target value of 1. The decreasing trend of the values of the weld dimensions is somewhat similar to that of arc efficiency. These trends are consistent with the fact that the arc efficiency has a major impact on the weld pool dimensions. Figures 3(*a*) and (*b*) show that the enhancement factor for the

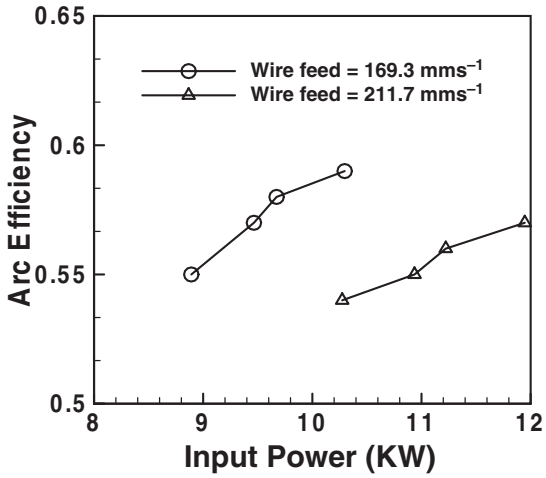

Figure 4. Computed values of the arc efficiency using the estimated values of the unknown parameters for the different welding conditions listed in table 1.

Table 2. Comparison of optimized values of the arc efficiency, η, effective thermal conductivity, k_e, and effective viscosity, μ_e, obtained using Fletcher and Reeves' CG method for the first eight welds listed in table 1.

No.	Heat input/length (KJ m^{-1})	η	k_e (J m^{-1} s^{-1} K^{-1})	μ_e (kg m^{-1} s^{-1})	Prandtl number
1	2302.8	0.58	112.9	0.04	0.29
2	1753.4	0.56	96.1	0.03	0.24
3	1608.7	0.59	92.0	0.03	0.23
4	2844.3	0.57	133.8	0.04	0.24
5	1389.2	0.55	87.8	0.03	0.28
6	2253.4	0.57	112.9	0.04	0.29
7	2446.0	0.54	121.2	0.04	0.26
8	1708.8	0.55	96.1	0.03	0.24

thermal conductivity and viscosity increases as the calculation progresses and the computed weld pool dimensions tend to agree progressively better with the corresponding experimental values. The optimal value of these unknown parameters can be expressed as

$$\eta = 0.31 + 4.65 \times 10^{-6} \frac{IV}{w_f}, \tag{1}$$

$$k_e = 41.80 + 3.17 \times 10^{-5} \frac{IV}{U_w} \text{ (W m}^{-1}\text{ K}^{-1}\text{)}, \tag{2}$$

$$\mu_e = 0.016 + 1.05 \times 10^{-8} \frac{IV}{U_w} \text{ (kg m}^{-1}\text{ s}^{-1}\text{)}, \tag{3}$$

where I is the current (A), V is the voltage (V), w_f is the wire feeding speed (m s^{-1}) and U_w is the welding speed (m s^{-1}). The values of η, k_e and μ_e calculated from equations (1), (2) and (3) can be used for the experimental conditions given in table 1 for GMA welding in the spray mode.

Figure 4 and table 2 show that the arc efficiency increases slightly with increasing input power and decreasing wire feeding rate (case #3 and case #8 of table 1). An approximately 8% increase in the value of the arc efficiency is observed with a decrease in the value of the wire feed rate from 211.7 to 169.3 mm s^{-1} for almost the same heat input/length (case #3 and case #8 of table 2). This behaviour is consistent with

the fact that with a decrease in wire feed rate, less power is consumed in melting the wire and more heat is available to the workpiece for the same heat input rate. Table 2 also shows that there can be 50% variation in the value of the effective thermal conductivity, depending on the heat input rate. Equations (2) and (3) show that the effective thermal conductivity and effective viscosity increase with increasing heat input per unit length. The increase in heat input rate enhances mixing in the weld pool and increases the effective thermal conductivity and viscosity. The optimized values indicate the enhancement factors (i.e. $f_k^e = k_e/k_L$) for the thermal conductivity and viscosity (i.e. $f_\mu^e = \mu_e/\mu_L$) to be in the range 5–9. This behaviour is consistent with the presence of turbulent flow in the weld pool during GMA welding as reported in [1, 2, 18–21]. Hong *et al* [19, 20] suggested an enhancement factor between 12 and 15 for thermal conductivity and a factor more than 6 for the viscosity for GTA welding using 150 A current and 25 V based on peak temperature analysis in the weld pool and k–ε turbulence model calculations. Choo and Szekely [18] suggested an enhancement factor of 8 for the thermal conductivity and a factor of 30 for the viscosity at a current of 100 A by matching the calculated weld pool geometry with the experimentally determined geometry. They also verified the weld pool shape and the values of the enhancement factors using the k–ε turbulence model. The values available in [3, 4, 15, 18–21] are specific to the welding procedure and the specific welding conditions. Because of the scarcity of data, the available literature cannot be used as a basis for the selection of enhanced transport parameters for any specific welding conditions.

The computed values of μ_e and k_e for various heat inputs indicate that the rates of transport of momentum and heat are considerably higher than for laminar flow. The relation between the two variables is governed by the turbulent Prandtl number (Pr), which is defined as

$$Pr = \frac{\mu_T c_P}{k_T}, \tag{4}$$

where $\mu_e = \mu_L + \mu_T$, $k_e = k_L + k_T$, μ_T and k_T are the turbulent viscosity and turbulent conductivity to account for the fluctuating fluid movement and resulting enhanced transport of heat and mass within the weld pool and c_P is the specific heat of the liquid. The values of Pr available in [16, 18] for a fully developed turbulent flow in molten alloys and steels are 0.9 and 0.2, respectively. The optimized values of μ_T and k_T obtained from Fletcher and Reeves' CG method result in Prandtl numbers between 0.2 and 0.3. These values of the Prandtl number lie between laminar and fully turbulent flow, which suggests that the flow in a GMAW fillet weld is neither laminar nor fully turbulent in the traditional sense for the welding conditions given in table 1. The structure of the flow in the weld pool is consistent with the need for enhanced values of transport properties for the heat transfer and fluid flow calculations.

2.3. Calculation of effective viscosity and thermal conductivity using mixing-length hypothesis

A vorticity-based mixing-length turbulence model has been used extensively for the calculation of the effective viscosity and effective thermal conductivity. In this model, the computational effort is significantly less compared with the k–ε turbulence model since it is algebraic in nature and does not require solution of any additional partial differential equations. Hong *et al* [15] implemented a vorticity-based turbulence model in their thermo-fluid calculation in the weld pool using a constant value of Prandtl mixing-length that was calculated by taking the ratio of the weld pool volume to its interfacial area. The constant mixing-length model cannot be applied to the finger-type penetration characteristic of the GMA fillet welding process, where the flow is constrained by the weld boundary which varies with the location. Therefore the mixing-length was calculated in this work using the Van Driest model [22, 23] which can accommodate local variation of the mixing-length in a weld pool of irregular geometry containing finger penetration. According to this model, the mixing-length at distance y from the weld pool boundary is given by

$$l_{mix} = \kappa y[1 - e^{-y^+/A_o^+}]. \tag{5}$$

The values of the constants κ and A_o^+ used in equation (5) are 0.41 and 26.0, respectively [22, 23], whereas the non-dimensional distance, y^+, from the weld pool boundary is calculated as follows [23]:

$$y^+ = y\sqrt{\frac{\rho}{\mu}\left(\frac{\partial u}{\partial y}\right)_w}. \tag{6}$$

The term $(\partial u/\partial y)_w$ in equation (6) represents the velocity gradient at the weld pool boundary. For the three-dimensional flow in the weld pool, the turbulent viscosity is calculated using the Badwin–Lomax model [22, 23] as follows:

$$\mu_T = \rho l_{mix}^2 |\omega|, \tag{7}$$

where $|\omega|$ is the magnitude of the vorticity vector given by

$$\omega = \left[\left(\frac{\partial v}{\partial x} - \frac{\partial u}{\partial y}\right)^2 + \left(\frac{\partial w}{\partial y} - \frac{\partial v}{\partial z}\right)^2 + \left(\frac{\partial u}{\partial z} - \frac{\partial w}{\partial x}\right)^2\right]^{1/2}. \tag{8}$$

The turbulent viscosity field is computed using equation (7) after every iteration. The corresponding turbulent thermal conductivity field is updated using a Pr value computed by the model. The calculated enhancement factor for viscosity ($f_\mu^e = 1 + \mu_T/\mu_L$) calculated using equation (7) for case #1 (table 1) is shown in figure 5. The results show that the enhanced viscosity is high under the arc while its value decreases in the rear part of the weld pool. The magnitude of the enhancement factor for viscosity is high under the arc due to the high spatial gradients of velocity in this region. The plane located 2 mm ahead of the arc shown in figure 5(*a*) is characterized by lower values of the enhanced viscosity compared with the region directly under the arc indicated in figure 5(*b*). The profiles of the viscosity enhancement factor in figures 5(*a*) and (*b*) clearly show the finger penetration characteristic of the GMA welding. From figure 5(*b*), it can be seen that the enhancement factor for viscosity is in the range 60–80 directly under the arc. The region further away and behind the arc has a relatively low enhanced viscosity as observed in figures 5(*c*) and (*d*) because of the low velocities.

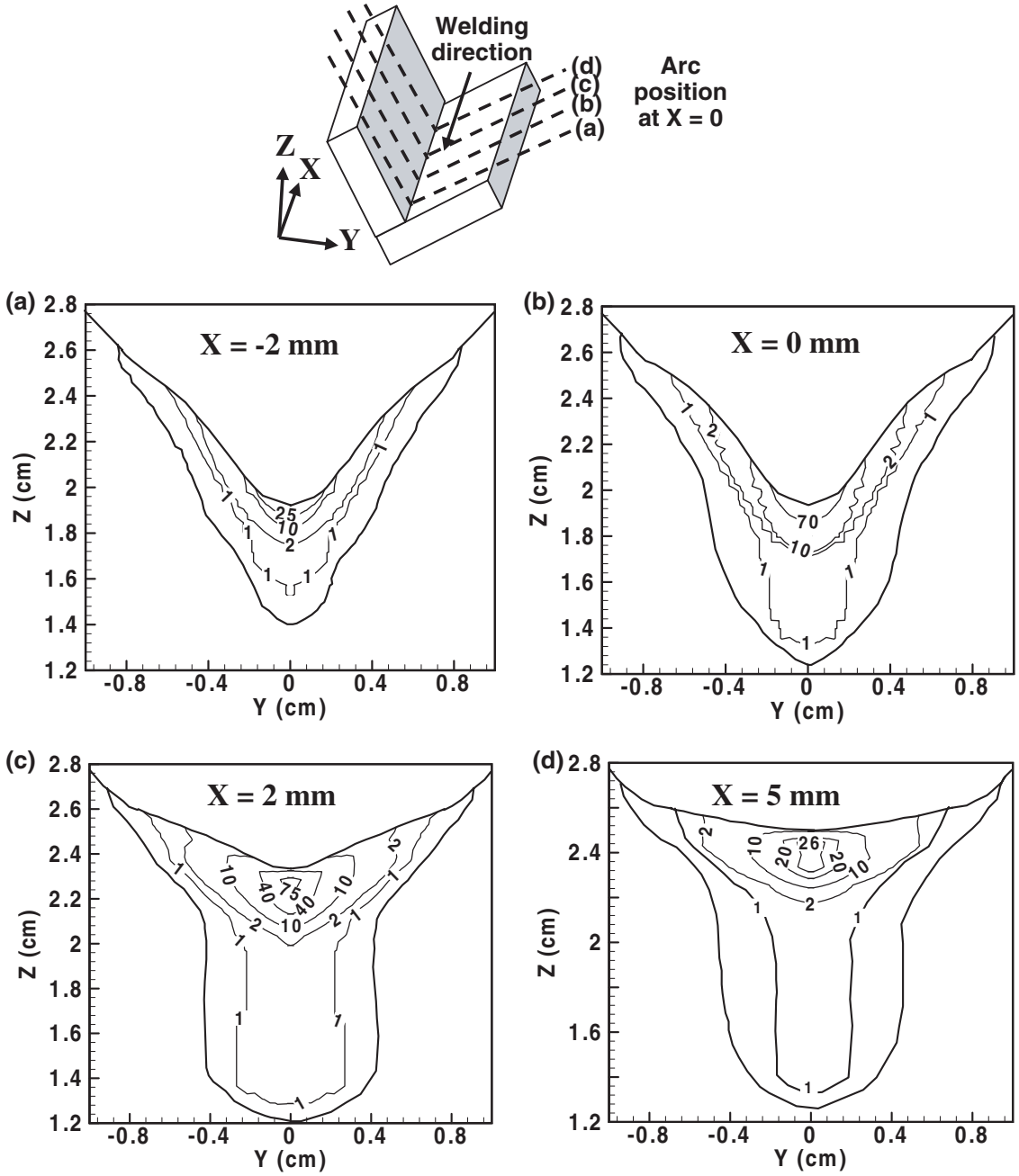

Figure 5. Calculated enhancement factor in viscosity using the mixing-length hypothesis on various planes perpendicular to the welding direction. The welding conditions are the same as those in case #1 (table 1): (*a*) 2 mm ahead of the arc location, (*b*) directly under the arc, (*c*) 2 mm behind the arc location and (*d*) 5 mm behind the arc location.

The average value of the enhancement factor for the viscosity in the weld pool was found to be 4.26 for the welding conditions indicated for weld #1 in table 1. The corresponding enhancement factor obtained from equation (3) is 5.24. This shows a reasonably good agreement between the values of the enhancement factor in the viscosity obtained by using the vorticity-based mixing-length turbulence model and the proposed equation (equation (3)). Using the effective viscosity of 4.26 and the *Pr* value (=0.29) obtained from the numerical heat transfer and fluid flow model for weld #1 in table 2, the enhancement factor for thermal conductivity was calculated. Figure 6 shows the calculated enhancement factors (i.e. $f_{\mathrm{k}}^{\mathrm{e}} = 1 + k_{\mathrm{T}}/k_{\mathrm{L}}$) for the thermal conductivity and viscosity (i.e. $f_{\mu}^{\mathrm{e}} = \mu_{\mathrm{e}}/\mu_{\mathrm{L}}$) as a function of the heat input using the vorticity-based turbulence model and the proposed equations (equations (2) and (3)). The calculated enhancement factors for the thermal conductivity and viscosity using vorticity-based turbulence also increase with increasing heat input per unit length as obtained from equations (2) and (3). The reasons for the slightly lower values of the average enhancement factors for the thermal conductivity and viscosity from the vorticity-based turbulence model compared with equations (2) and (3) are not known. However, the fact that the values of the constants κ and A_{o}^{+} in equation (5) were obtained

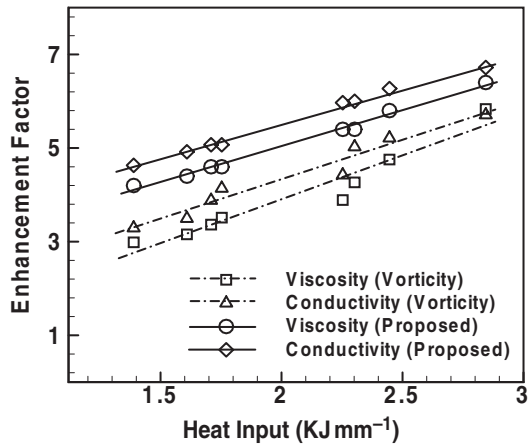

Figure 6. Computed values of the enhancement factor for the thermal conductivity and viscosity using the estimated values of the unknown parameters using the proposed model and the vorticity-based turbulence model for the different welding conditions listed in table 1.

from experiments in parabolic flows may be a contributing factor.

Figures 7(*a*), (*b*) and (*c*) show a comparison between the computed and the experimentally obtained weld pool dimensions using the optimized values of the arc efficiency, effective thermal conductivity and effective viscosity obtained from equations (1)–(3) for the welding conditions listed in table 1. These figures show a satisfactory agreement between the computed and experimentally obtained weld geometries for various welding conditions. The reliability of the numerical heat transfer and fluid flow calculations can be significantly enhanced by using the optimized values of the uncertain welding parameters from a limited volume of measured weld dimensions.

3. Summary and conclusions

A model for GMA fillet welding involving numerical calculation of the heat transfer and fluid flow and multiple parameter optimization was developed. This model could estimate the unknown values of the arc efficiency, effective thermal conductivity and effective viscosity based on only a few experimental measurements. The optimized values of the arc efficiency, effective thermal conductivity and effective viscosity were found to depend on the welding conditions. The enhancement factors for the thermal conductivity and viscosity were in the range 5–9 for the welding conditions used in this study. The manner in which the effective viscosity and effective thermal conductivity vary in the weld pool was also analysed using a vorticity-based mixing-length turbulence model. This proposed vorticity-based turbulence model uses a variable mixing-length to capture the effect of the weld pool boundary on the fluid flow in the weld pool. The average values of the enhancement factors for the thermal conductivity and viscosity calculated using the vorticity-based mixing-length turbulence model agreed well with the values predicted by the proposed model. The reliability of the numerical heat transfer and fluid flow calculations in the weld pool can be significantly improved by including a suitable optimization

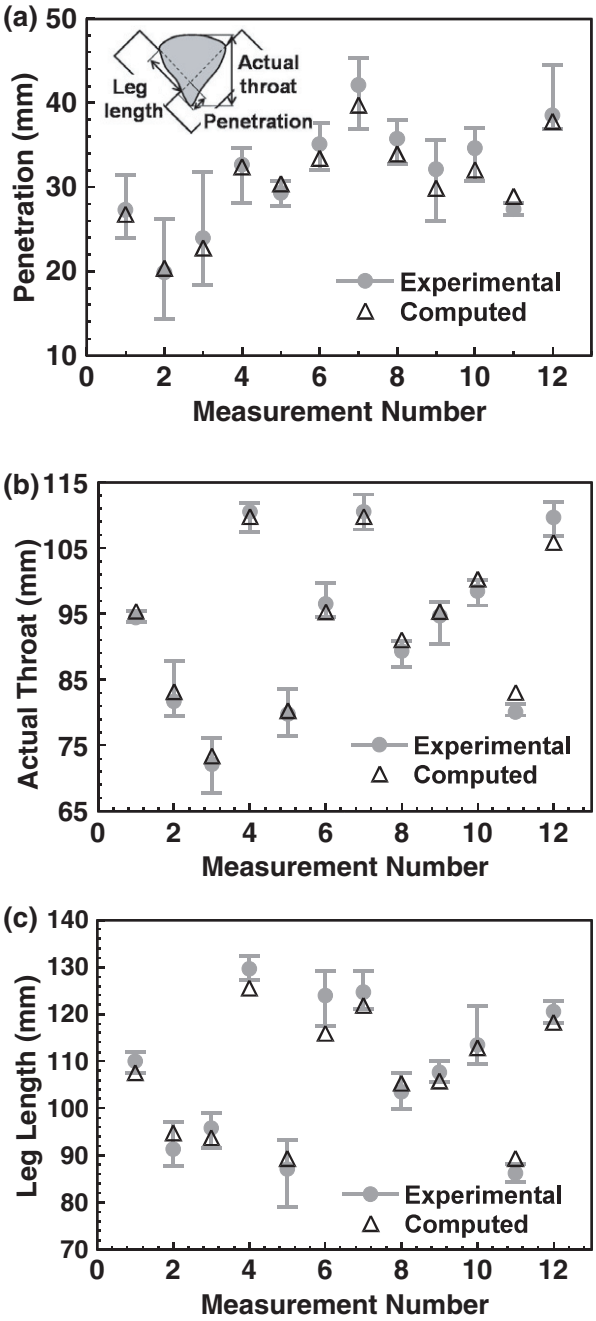

Figure 7. Comparison between the computed and experimental values of (*a*) penetration, (*b*) actual throat and (*c*) leg length obtained using the optimized value of the arc efficiency, effective thermal conductivity and effective viscosity for all the conditions listed in table 1.

model to determine the uncertain welding parameters from a limited volume of experimental data on weld dimensions.

Acknowledgments

This research was supported by a grant from the US Department of Energy, Office of Basic Energy Sciences, Division of Materials Sciences, under grant number DE-FGO2-01ER45900. The authors thank S Mishra and X He for their useful comments on the manuscript.

References

[1] Zhang W, Kim C H and DebRoy T 2004 *J. Appl. Phys.* **95** 5210
[2] Zhang W, Kim C H and DebRoy T 2004 *J. Appl. Phys.* **95** 5220
[3] De A and DebRoy T 2004 *J. Phys. D: Appl. Phys.* **37** 140
[4] De A and DebRoy T 2004 *J. Appl. Phys.* **95** 5230
[5] Zhang W, Roy G, Elmer J W and DebRoy T 2003 *J. Appl. Phys.* **93** 3022
[6] Kumar A and DebRoy T 2003 *J. Appl. Phys.* **94** 1267
[7] He X, Fuerschbach P W and DebRoy T 2003 *J. Phys. D: Appl. Phys.* **36** 1388
[8] He X, Fuerschbach P W and DebRoy T 2003 *J. Phys. D: Appl. Phys.* **36** 3079
[9] Zhao H, White D R and DebRoy T 1999 *Int. Mater. Rev.* **44** 238
[10] Zhao H and DebRoy T 2003 *J. Appl. Phys.* **93** 10089
[11] Zhao H and DebRoy T 2001 *Metall. Mater. Trans.* B **32** 163
[12] Elmer J W, Palmer T A, Babu S S, Zhang W and DebRoy T 2004 *J. Appl. Phys.* **95** 8327
[13] Mishra S and DebRoy T 2004 *J. Phys. D: Appl. Phys.* **37** 2191
[14] Hong T and DebRoy T 2001 *Ironmaking Steelmaking* **28** 450
[15] Hong K, Weckmann D C, Strong A B and Zheng W 2003 *Sci. Technol. Weld. Joining* **8** 313
[16] Szekely J 1979 *Fluid Flow Phenomena in Material Processing* (New York: Academic)
[17] Kumar A and DebRoy T 2004 *Int. J. Heat Mass Transfer* **47** 5789
[18] Choo R T C and Szekely J 1994 *Weld. J.* **73** 25
[19] Hong K, Weckmann D C, Strong A B and Zheng W 2002 *Sci. Technol. Weld. Joining* **7** 125
[20] Hong K, Weckman D C, Strong A B and Pardo E 1992 *Proc. First Int. Conf. on Transport Phenomena in Processing (Hawaii)* ed S I Guceri (Lancaster, PA: Technomic Pub.) p 626
[21] Jonsson P G, Szekely J, Choo R T C and Quinn T P 1994 *Modelling Simul. Mater. Sci. Eng.* **2** 995
[22] Wilcox D C 1993 *Turbulence Modeling for CFD* (California: DCW Industries)
[23] Launder B E and Spalding D B 1972 *Lectures in Mathematical Models of Turbulence* (London: Academic)